Targeting of cathepsin S reduces cystic fibrosis-like lung disease

Donna M. Small[1,10], Ryan R. Brown[1,10], Declan F. Doherty[1], Anthony Abladey[1], Zhe Zhou-Suckow[2], Rebecca J. Delaney[1], Lauren Kerrigan[1], Caoifa M. Dougan[1], Keren S. Borensztajn[3], Leslie Holsinger[4], Robert Booth[4], Christopher J. Scott[5], Guillermo López-Campos[6], J. Stuart Elborn[6,7], Marcus A. Mall[2,8,9], Sinéad Weldon[1] and Clifford C. Taggart[1]

Affiliations: [1]Airway Innate Immunity Research (AiiR) Group, Wellcome-Wolfson Institute for Experimental Medicine, School of Medicine, Dentistry and Biomedical Sciences, Queen's University Belfast, Belfast, UK. [2]Dept of Translational Pulmonology, Translational Lung Research Center Heidelberg (TLRC), German Center for Lung Research (DZL), University of Heidelberg, Heidelberg, Germany. [3]INSERM UMRS_933, Université Pierre et Marie Curie, Hôpital Trousseau, Paris, France. [4]ViroBay Inc., Menlo Park, CA, USA. [5]Centre for Cancer Research and Cell Biology, Queen's University Belfast, Belfast, UK. [6]Wellcome-Wolfson Institute for Experimental Medicine, School of Medicine, Dentistry and Biomedical Sciences, Queen's University Belfast, Belfast, UK. [7]Respiratory Medicine, Imperial College and Royal Brompton Hospital, London, UK. [8]Dept of Pediatric Pulmonology and Immunology, Charité – Universitätsmedizin Berlin, Berlin, Germany. [9]Berlin Institute of Health (BIH), Berlin, Germany. [10]These two authors contributed equally to this work.

Correspondence: Sinéad Weldon, Airway Innate Immunity Research (AiiR) Group, Wellcome-Wolfson Institute for Experimental Medicine, School of Medicine, Dentistry and Biomedical Sciences, Queen's University Belfast, 97 Lisburn Road, Belfast, BT9 7BL, UK. E-mail: s.weldon@qub.ac.uk

ABSTRACT Cathepsin S (CatS) is upregulated in the lungs of patients with cystic fibrosis (CF). However, its role in CF lung disease pathogenesis remains unclear.

In this study, β-epithelial Na^+ channel-overexpressing transgenic (βENaC-Tg) mice, a model of CF-like lung disease, were crossed with CatS null (CatS$^{-/-}$) mice or treated with the CatS inhibitor VBY-999.

Levels of active CatS were elevated in the lungs of βENaC-Tg mice compared with wild-type (WT) littermates. CatS$^{-/-}$βENaC-Tg mice exhibited decreased pulmonary inflammation, mucus obstruction and structural lung damage compared with βENaC-Tg mice. Pharmacological inhibition of CatS resulted in a significant decrease in pulmonary inflammation, lung damage and mucus plugging in the lungs of βENaC-Tg mice. In addition, instillation of CatS into the lungs of WT mice resulted in inflammation, lung remodelling and upregulation of mucin expression. Inhibition of the CatS target, protease-activated receptor 2 (PAR2), in βENaC-Tg mice resulted in a reduction in airway inflammation and mucin expression, indicating a role for this receptor in CatS-induced lung pathology.

Our data indicate an important role for CatS in the pathogenesis of CF-like lung disease mediated in part by PAR2 and highlight CatS as a therapeutic target.

Introduction

Cathepsin S (CatS) is expressed by professional and nonprofessional antigen-presenting cells, and is a crucial component in major histocompatibility complex class II antigen processing and presentation [1]. CatS is a potent elastinolytic and collagenolytic cysteine protease with the ability to maintain its enzymatic activity in more neutral pH environments [2, 3]. Previous work has demonstrated that levels of CatS are elevated in lungs of patients with cystic fibrosis (CF) lung disease [4–7] and chronic obstructive pulmonary disease (COPD) [8], and that CatS correlates significantly with a decline in lung function and increased pulmonary neutrophilic infiltration into the CF lung [7]. Furthermore, CatS possesses the ability to cleave and inactivate host defence proteins such as lactoferrin, β-defensins, LL-37, secretory leukoprotease inhibitor and surfactant protein A [4, 9–12], which may increase susceptibility to infection in patients with these muco-obstructive lung diseases.

However, the role of CatS in CF lung disease pathobiology has yet to be fully elucidated. In this study we employed a mouse model of CF-like lung disease to investigate the functionality of CatS *in vivo*. Overexpression of the β subunit of the epithelial Na^+ channel (βENaC) results in airway surface dehydration and impaired mucus clearance, producing chronic lung disease characterised by airway mucus obstruction, inflammation and structural lung damage in mice [13]. Therefore, the βENaC-overexpressing transgenic (βENaC-Tg) mouse model shares many characteristics with human CF, and is a useful *in vivo* model to study the role and therapeutic potential of CatS in CF-like lung disease [14].

Following demonstration that elevated CatS levels and activity were a feature of the βENaC-Tg lung, we crossed βENaC-Tg mice onto a CatS null (CatS$^{-/-}$) background and assessed airway inflammation, mucus obstruction and lung damage. To validate observations in this model we also investigated the effects of therapeutic targeting of CatS *via* a small-molecule inhibitor in the diseased lung. In addition, we instilled CatS directly into the lungs of wild-type (WT) mice to investigate effects on inflammatory cell recruitment, mucin production and lung remodelling. To further understand how CatS functions in the lung, we assessed the role of the protease-activated receptor 2 (PAR2), a target for CatS [15–20], in mediating the effects of CatS in βENaC-Tg mice.

Methods

Full details are available in the supplementary methods.

Abbreviated methods

All experimentation was carried out in accordance with the Animal (Scientific Procedures) Act 1986 and current guidelines approved by the Ethical Review Committee of Queen's University Belfast (Belfast, UK).

All mice used in this study were from a C57BL/6 background. This breeding programme generated four genotypes of mice for investigation: WT, CatS$^{-/-}$, βENaC-Tg and CatS$^{-/-}$βENaC-Tg mice. Offspring were genotyped by PCR as previously described [13, 21, 22] and mice were used from the newborn stage. Newborn βENaC-Tg mice and WT littermates were dosed once daily for 14 days *via* a subcutaneous injection of the CatS inhibitor VBY-999 (100 mg·kg^{-1}; Virobay, Menlo Park, CA, USA), the selective PAR2 peptide antagonist FSLLRY-NH$_2$ (4 mg·kg^{-1}; R&D Systems, Abingdon, UK) or their respective vehicle controls, *i.e.* dextrose solution and sterile water. WT mice were intratracheally instilled with recombinant human CatS (rhCatS, 5 µg; Merck Millipore, Nottingham, UK). Bronchoalveolar lavage (BAL) fluid was collected for analysis of inflammatory markers and cell recruitment as previously described [13, 23]. Histological staining and morphometric assessments of airspace enlargement, alveolar wall destruction and airway mucus content were conducted as previously described [24–26].

Results

Upregulation of CatS in the lungs of βENaC-Tg mice

In order to validate the βENaC-Tg mouse model as a suitable model to test the effects of targeting CatS, we determined the status of CatS levels and activity in βENaC-Tg mice. We observed increased levels of CatS protein (figure 1a) and CatS activity (figure 1b) in BAL fluid from βENaC-Tg mice compared with healthy WT counterparts. In addition, we observed increased CatS staining in βENaC-Tg mouse lungs, which was primarily localised to macrophages, with some epithelial staining also present (figure 1c). These findings demonstrate that, like human CF, increased levels of active CatS are a feature of the βENaC-Tg mouse model.

Genetic ablation of CatS results in decreased pulmonary inflammation in βENaC-Tg mice

In order to investigate the role of CatS in the pathogenesis of CF-like lung disease, we first assessed pulmonary inflammation in CatS$^{-/-}$βENaC-Tg, βENaC-Tg and control mice (CatS$^{-/-}$ and WT littermates). There was no significant change in BAL fluid total cell numbers in CatS$^{-/-}$ compared with WT control mice (figure 2a). As expected, βENaC-Tg mice demonstrated significantly increased cell infiltration compared with
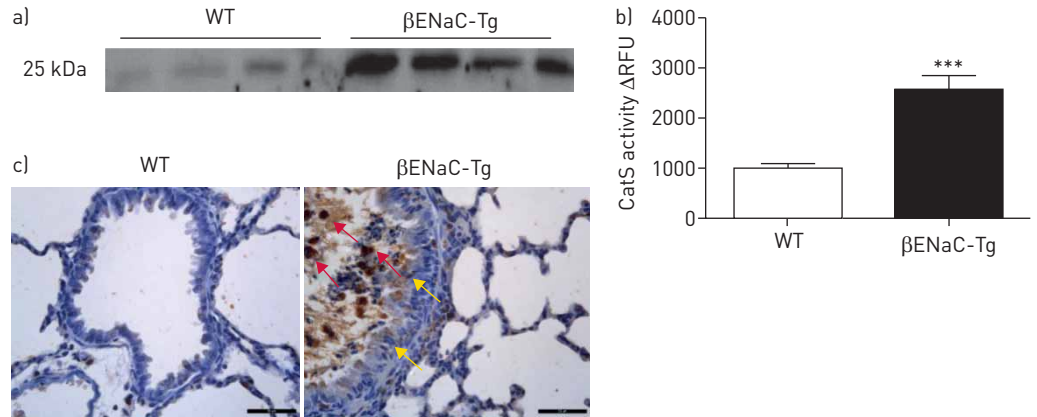
FIGURE 1 Levels and activity of cathepsin S (CatS) are upregulated in the lungs of β-epithelial Na⁺ channel-overexpressing transgenic (βENaC-Tg) mice. WT: wild-type; RFU: relative fluorescence units; BAL: bronchoalveolar lavage. a) Western blot of CatS in BAL fluid from βENaC-Tg and WT mice. n=4 per group. b) CatS activity in BAL fluid from WT and βENaC-Tg mice was determined using Z-Phe-Arg-7-amido-4-methylcoumarin, hydrochloride substrate (pH 7.5). Results are presented as ΔRFU over time. n=10 per group. ***: p<0.001. c) Immunohistochemical staining for CatS on lung sections from WT and βENaC-Tg mice. Red arrows: macrophage CatS staining; yellow arrows: epithelial CatS staining.
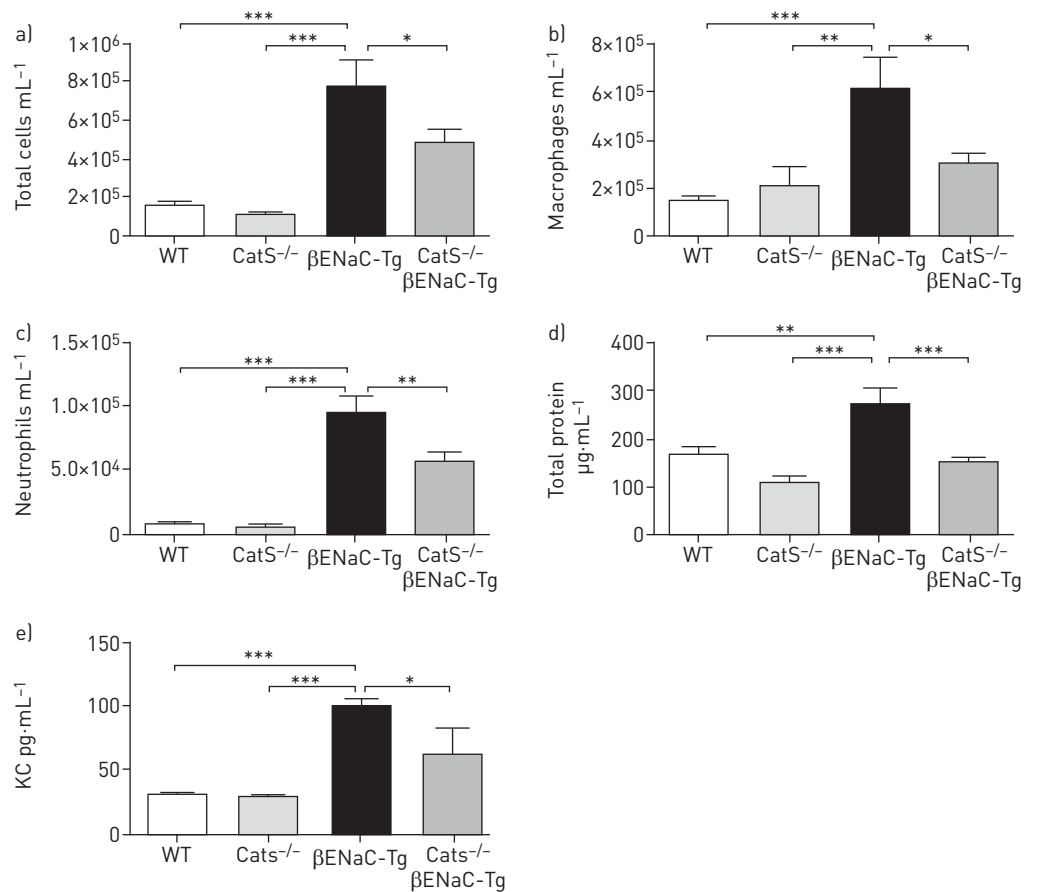

FIGURE 2 Genetic ablation of cathepsin S (CatS) reduces airway inflammation in β-epithelial Na⁺ channel-overexpressing transgenic (βENaC-Tg) mice. WT: wild-type; BAL: bronchoalveolar lavage. βENaC-Tg mice were crossed with CatS⁻/⁻ mice to produce CatS⁻/⁻βENaC-Tg mice. BAL fluid was collected from WT, CatS⁻/⁻, βENaC-Tg and CatS⁻/⁻βENaC-Tg mice. BAL a) total cell, b) macrophage and c) neutrophil counts, and d) total protein concentration were quantified. n=7–10 per group. e) BAL fluid levels of chemokine KC were assessed by ELISA. n=5–7 per group. *: p<0.05; **: p<0.01; ***: p<0.001.

WT and CatS$^{-/-}$ mice (figure 2a). CatS$^{-/-}$βENaC-Tg mice BAL total cell counts were significantly decreased compared with βENaC-Tg mice (figure 2a) as evidenced by a reduction in both macrophage (figure 2b) and neutrophil (figure 2c) cell populations. BAL fluid total protein concentrations were significantly higher in βENaC-Tg mice compared with control mice (figure 2d). However, total protein content was significantly reduced in CatS$^{-/-}$βENaC-Tg mice compared with βENaC-Tg mice, suggesting a reduction in the severity of lung damage and inflammation (figure 2d). In addition, we observed significantly decreased levels of the chemokine KC (figure 2e) in BAL fluid of CatS$^{-/-}$βENaC-Tg mice compared with βENaC-Tg mice.

Genetic ablation of CatS results in decreased structural lung damage and mucus obstruction in the lungs of βENaC-Tg mice

Mean linear intercept length (L_m) is a measurement of distal airspace enlargement. Airway sections stained with haematoxylin and eosin (representative images shown in figure 3a) demonstrated no difference in L_m between CatS$^{-/-}$ and WT mice (figure 3b). As expected, a significant increase in L_m was evident in the lungs of βENaC-Tg mice compared with control mice (figure 3b). In comparison with βENaC-Tg mice, L_m was significantly reduced in CatS$^{-/-}$βENaC-Tg mice (figure 3b), suggesting that increased CatS in the lungs of βENaC-Tg mice may play a role in distal airspace enlargement. In addition, the level of alveolar septal destruction, as assessed by measurement of the destructive index (DI), was significantly reduced in CatS$^{-/-}$βENaC-Tg mice compared with βENaC-Tg mice, with no difference in DI measurements observed between WT and CatS$^{-/-}$ control mice (figure 3c). Given the levels of airspace enlargement and damage observed, these findings indicate that the augmented CatS levels found in βENaC-Tg may play an important role in mediating lung tissue damage and remodelling in CF-like lung disease. Histological staining and quantification of airway mucus content demonstrated a significant reduction in airway mucus
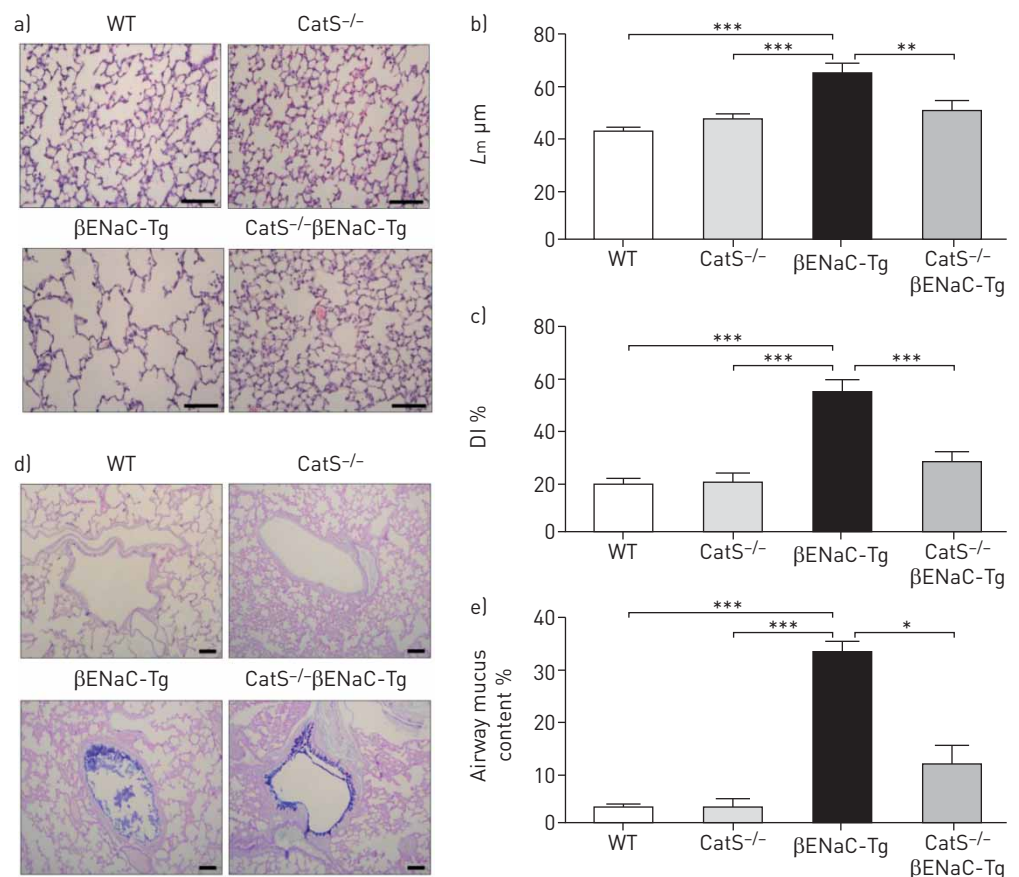

FIGURE 3 Lack of cathepsin S (CatS) in β-epithelial Na$^+$ channel-overexpressing transgenic (βENaC-Tg) mice reduces airway mucus obstruction and lung tissue damage. WT: wild-type; HE: haematoxylin and eosin; L_m: mean linear intercept length; DI: destructive index. a) Representative images of lung sections from WT, CatS$^{-/-}$, βENaC-Tg and CatS$^{-/-}$βENaC-Tg mice stained with HE used to assess airway damage. Scale bar: 100 µm. b) L_m and c) DI measurements were assessed from the HE-stained lung sections. d) Representative images of lung sections stained with Alcian Blue–Periodic acid–Schiff. Scale bar: 100 µm. e) Airway mucus quantification expressed as percentage of the total airway containing mucus. n=7–10 per group. *: p<0.05; **: p<0.01; ***: p<0.001.

obstruction in CatS$^{-/-}$βENaC-Tg mice compared with βENaC-Tg mice (figure 3d and e). Overall, these findings suggest that CatS is implicated in the pathogenesis of chronic inflammation, lung tissue damage and the development of mucus plugging in CF-like lung disease.

Pharmacological inhibition of CatS reduces airway inflammation in βENaC-Tg mice

CatS was targeted using a small-molecule inhibitor, VBY-999 [27], in βENaC-Tg mice. Inhibition of CatS alters invariant chain (Ii) processing and results in the accumulation of the 10 kDa intermediate (p10) [1, 22]. To determine whether VBY-999 was successfully targeting CatS in the lung, we assessed the accumulation of the Ii p10 fragment by Western blotting. The lungs of βENaC-Tg mice treated with VBY-999 exhibited an accumulation of Ii p10 levels compared with vehicle (dextrose)-treated βENaC-Tg mice (figure 4a). Initially, we observed that βENaC-Tg mice treated with VBY-999 from birth for a period of 14 days demonstrated a significant increase in survival compared with dextrose-treated mice (supplementary figure S1). βENaC-Tg mice treated with VBY-999 had significantly lower BAL total inflammatory cellular infiltrate compared with vehicle-treated βENaC-Tg mice (figure 4b). There was no effect on total cell numbers in the control mice regardless of treatments. VBY-999 treatment significantly decreased the number of BAL macrophages (figure 4c) and neutrophils (figure 4d) in βENaC-Tg mice. In addition, we observed significantly decreased levels of KC (figure 4e) in BAL fluid of VBY-999-treated βENaC-Tg mice compared with vehicle-treated βENaC-Tg mice. These data suggest that inhibition of CatS suppresses pulmonary inflammation in this mouse model of CF-like lung disease.

Inhibition of pulmonary CatS reduces the level of structural lung damage and lung protein content in βENaC-Tg mice

Protein levels were assessed by BCA (bicinchoninic acid) assay and VBY-999-treated βENaC-Tg mice had lower levels of total protein in BAL fluid compared with vehicle-treated βENaC-Tg mice (figure 5a). L_m
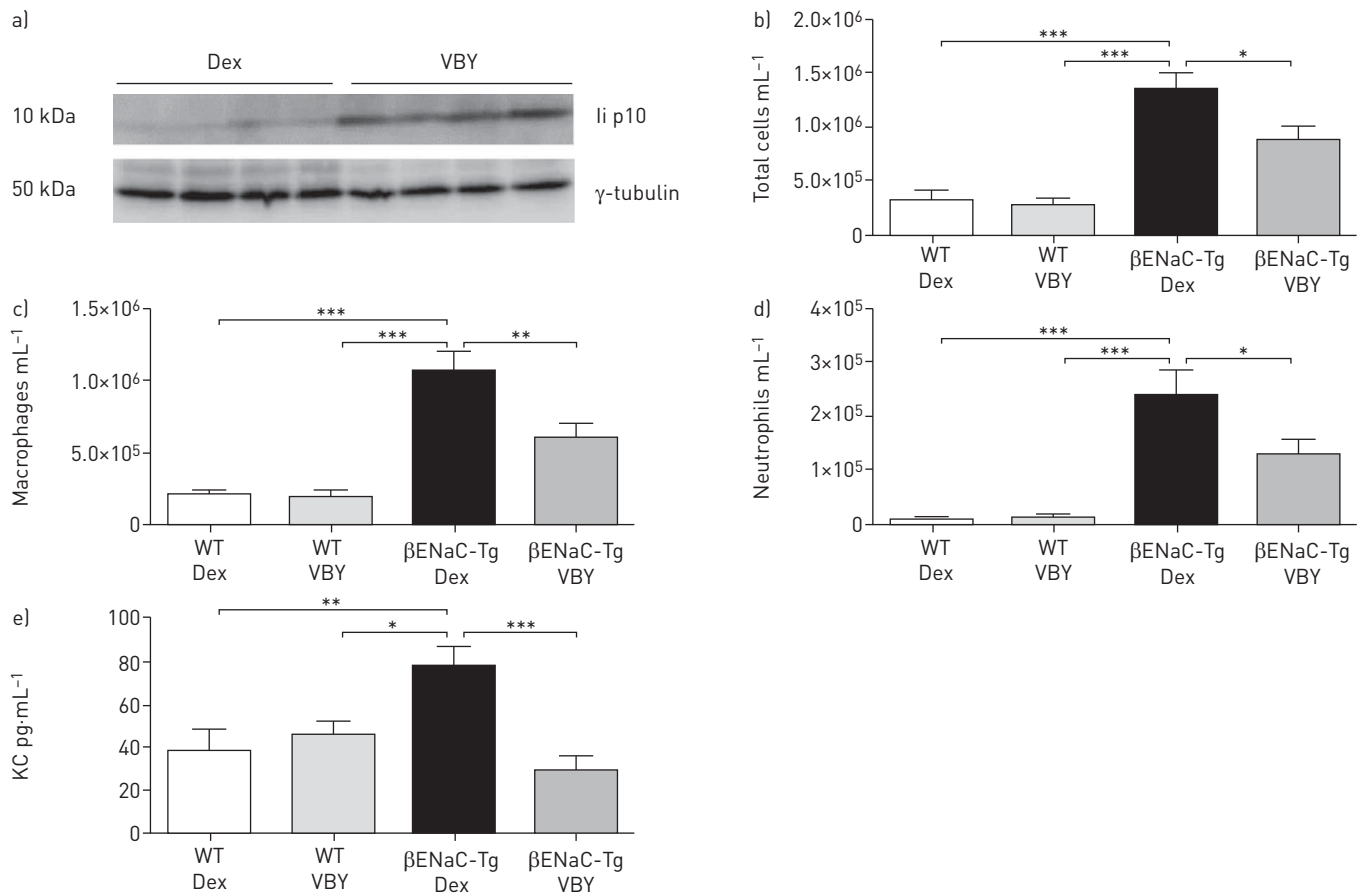

FIGURE 4 Pharmacological targeting of cathepsin S (CatS) leads to a reduction in pulmonary inflammation in β-epithelial Na$^+$ channel-overexpressing transgenic (βENaC-Tg) mice. Dex: dextrose; VBY: VBY-999; Ii: invariant chain; WT: wild-type; BAL: bronchoalveolar lavage. WT and βENaC-Tg mice were treated daily with the CatS inhibitor VBY (100 mg·kg^{-1}) or vehicle control (Dex) for 14 days. a) Western blot of Ii p10 in lung homogenate from Dex- and VBY-treated βENaC-Tg mice. n=4 per group. BAL b) total cell, c) macrophage and d) neutrophil counts were quantified. n=10–15 per group. e) BAL fluid levels of chemokine KC were assessed by ELISA. n=9–15 per group. *: p<0.05; **: p<0.01; ***: p<0.001.
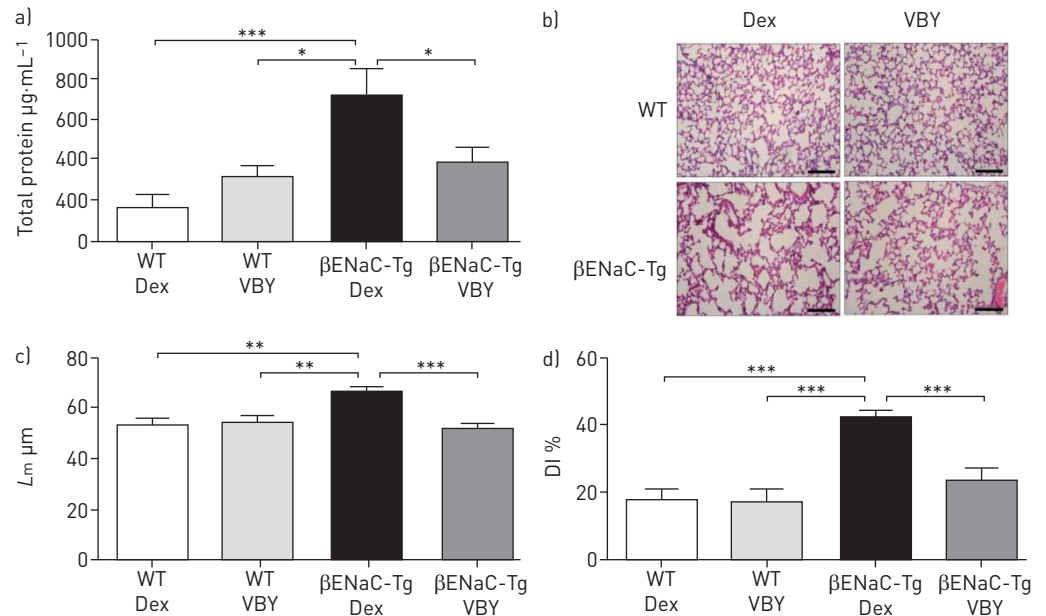
FIGURE 5 Cathepsin S (CatS) inhibition reduces airway tissue damage in β-epithelial Na$^+$ channel-overexpressing transgenic (βENaC-Tg) mice. WT: wild-type; Dex: dextrose; VBY: VBY-999; BAL: bronchoalveolar lavage; BCA: bicinchoninic acid; HE: haematoxylin and eosin; L_m: mean linear intercept length; DI: destructive index. WT and βENaC-Tg mice were treated daily with the CatS inhibitor VBY (100 mg·kg^{-1}) or vehicle control (Dex) for 14 days. a) BAL fluid protein levels were quantified by BCA assay. n=7–8 per group. b) Representative images of lung sections stained with HE used to assess airway damage. Scale bar: 100 µm. c) L_m and d) DI measurements were assessed from the HE-stained lung sections. n=6–7 per group. *: p<0.05; **: p<0.01; ***: p<0.001.

and DI were measured using haematoxylin and eosin-stained lung sections from each group (figure 5b) as markers of airspace enlargement and alveolar destruction, respectively. There was a significant decrease in L_m in βENaC-Tg mice treated with VBY-999 compared with vehicle (figure 5c). Additionally, a significant decline in alveolar wall destruction was observed in VBY-999-treated βENaC-Tg mice compared with vehicle-treated βENaC-Tg mice (figure 5d). These data demonstrate that inhibition of CatS resulted in a reduction in airway damage in CF-like lung disease.

Inhibition of CatS results in reduced airway mucus content in βENaC-Tg mice
Histological analyses demonstrated that VBY-999-treated βENaC-Tg mice presented with a significant decrease in airway mucus content compared with dextrose-treated βENaC-Tg mice (figure 6a and b). Given our previous findings of altered mucus content in CatS$^{-/-}$βENaC-Tg mice (figure 3d and e), we investigated the expression of the mucins Muc5ac and Muc5b and the goblet cell marker Gob5 (figure 6c–e). Treatment of βENaC-Tg mice with VBY-999 from birth significantly reduced the expression levels of *Muc5ac* (figure 6c) and *Gob5* (figure 6e) compared with dextrose-treated βENaC-Tg mice. In contrast, inhibition of CatS had no effect on the expression level of *Muc5b* (figure 6d).

Effect of CatS pulmonary instillation on lung inflammation and mucin production
Direct instillation of rhCatS into the lungs of WT mice induced significant recruitment of inflammatory cells (figure 7a), largely attributed to the influx in macrophages (figure 7b) and neutrophils (figure 7c). Although there was a significant increase in the expression levels of *Muc5ac* (figure 7d) and *Gob5* (figure 7e) in the lungs of mice that received CatS, the expression level of *Muc5b* was unchanged (figure 7f). In addition, rhCatS administration was associated with goblet cell hyperplasia (figure 7g–i). KC levels in BAL fluid (figure 7j) were significantly increased following rhCatS instillation and evidence of lung damage was also observed with significantly increased levels of the elastin breakdown product, desmosine, detectable in the lungs of CatS-treated mice (figure 7k).

CatS-induced lung inflammation and mucin expression is mediated in part via PAR2
CatS has previously been shown to activate the receptor PAR2, leading to symptoms of inflammation, itch and pain, and has been associated with conditions such as atopic dermatitis and colitis as well as endothelial dysfunction associated with lupus nephritis and diabetes [15–20]. However, a role for PAR2 in
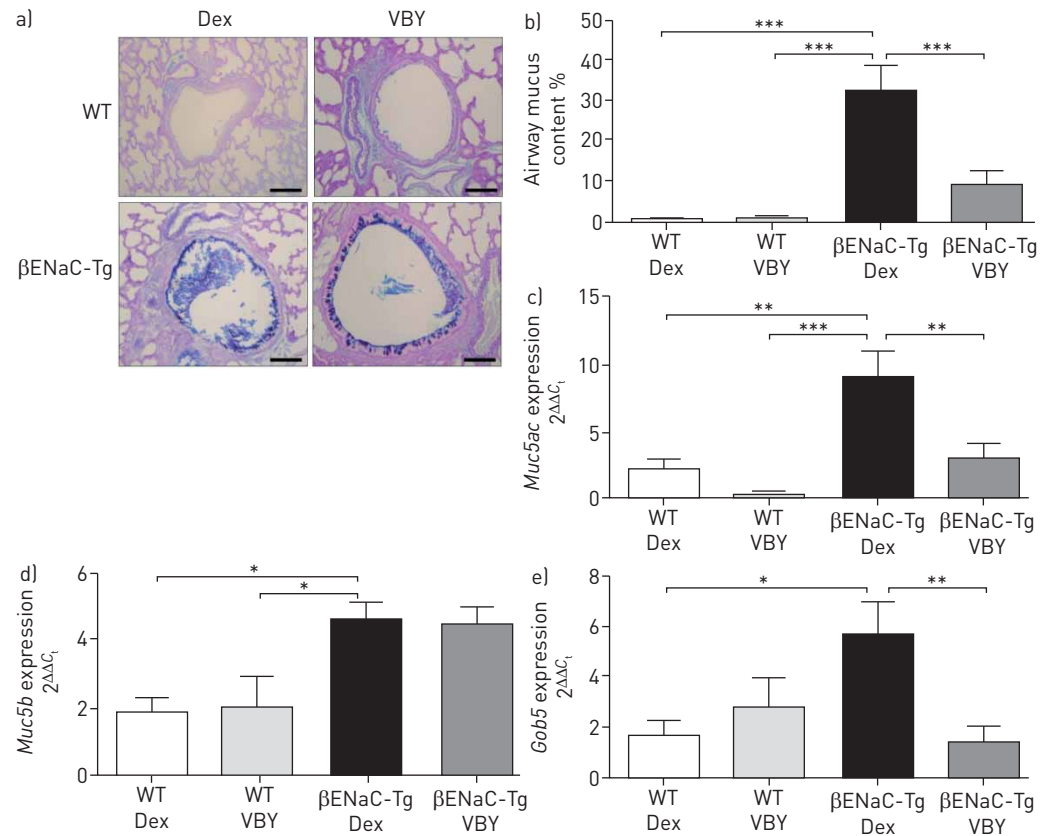
FIGURE 6 Pharmacological targeting of cathepsin S (CatS) reduces airway mucus plugging and mucin gene expression in β-epithelial Na⁺ channel-overexpressing transgenic (βENaC-Tg) mice. Dex: dextrose; VBY: VBY-999; WT: wild-type. WT and βENaC-Tg mice were treated daily with the CatS inhibitor VBY (100 mg·kg^{-1}) or vehicle control (Dex) for 14 days. a) Representative images of lung sections from WT and βENaC-Tg mice treated with Dex or VBY stained with Alcian Blue–Periodic acid–Schiff to assess airway mucus content. Scale bar: 100 μm. b) Airway mucus quantification in WT and βENaC-Tg mice treated with Dex or VBY. Results are presented as percentage of the total airway area containing mucus. n=9–13 per group. Expression levels of c) Muc5ac, d) Muc5b and e) Gob5 in lung tissue were analysed by quantitative PCR. n=6–14 per group. *: p<0.05; **: p<0.01; ***: p<0.001.

CatS-mediated lung inflammation or mucin expression *in vivo* has not been described to date. Treatment of WT mice with a PAR2 antagonist (FSLLRY-NH$_2$) reduced the infiltration of inflammatory cells into the lungs of rhCatS-treated mice (supplementary figure S2). Therefore, the impact of a PAR2 antagonist in the βENaC-Tg mouse lung was evaluated. Similar to genetic and pharmacological inhibition of CatS, blockade of PAR2 in βENaC-Tg mice led to a significant reduction in lung inflammation, with a decline in total inflammatory cell lung infiltrate (figure 8a), macrophages (figure 8b) and neutrophils (figure 8c) in the lungs of βENaC-Tg mice compared with vehicle (sterile water)-treated βENaC-Tg mice. In addition, BAL fluid KC levels were significantly decreased in PAR2 antagonist-treated βENaC-Tg mice compared with vehicle-treated βENaC-Tg mice (figure 8d). The expression levels of Muc5ac and Gob5 (figure 8e and f) were decreased in the lungs of PAR2 antagonist-treated βENaC-Tg mice compared with vehicle-treated βENaC-Tg mice. However, there was no reduction in the level of airspace enlargement or alveolar destruction as measured by *L*m and DI, respectively (data not shown). Overall, these data indicate a significant role for PAR2 in CatS-mediated lung inflammation and mucus production in the lungs of βENaC-Tg mice.

Discussion

CatS is elevated in a number of muco-inflammatory conditions like CF lung disease and COPD, and is viewed as a potential therapeutic target for various diseases (recently reviewed in [28, 29]). We have previously shown that increased CatS activity in the CF lung is associated with a decline in lung function [7]. In addition, pulmonary CatS levels and activity significantly correlated with neutrophilic infiltration in the CF lung [7], substantiating the hypothesis that CatS may play a role in pulmonary neutrophil recruitment [30], which is associated with CF lung disease. In the current study, we show that elevated
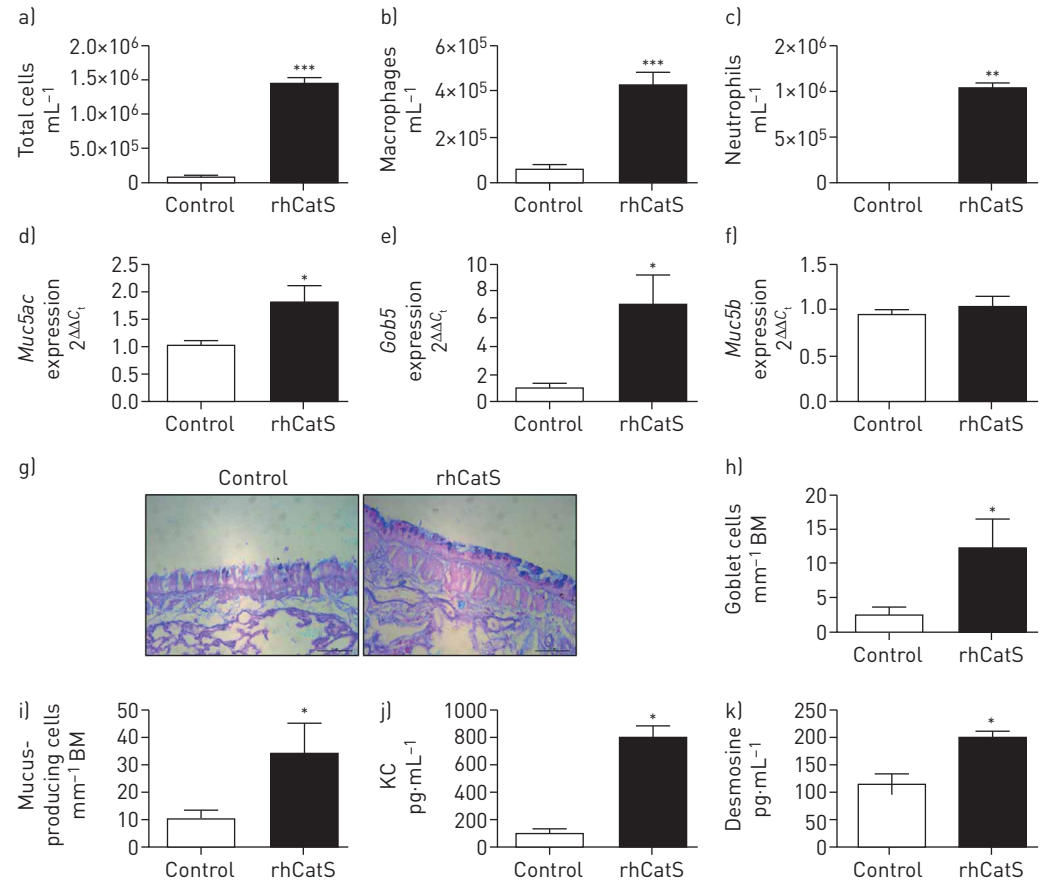
FIGURE 7 Cathepsin S (CatS) instillation induces inflammation and mucus in the lungs. rhCatS: recombinant human CatS; BM: basement membrane; WT: wild-type; BAL: bronchoalveolar lavage; AB-PAS: Alcian Blue–Periodic acid–Schiff. WT mice received a single intratracheal instillation of rhCatS (5 µg) or sodium acetate buffer control. After 24 h, BAL fluid was collected, and a) total cell, b) macrophage and c) neutrophil counts were quantified. Expression levels of d) Muc5ac, e) Gob5 and f) Muc5b in lung tissue were analysed by quantitative PCR. g) Representative images of lung sections stained with AB-PAS. Scale bar: 50 µm. h) Goblet and i) mucus-producing cells were quantified from AB-PAS-stained lung sections. Results are presented as cells·mm^{-1} BM. BAL fluid j) chemokine KC and k) desmosine levels were assessed by ELISA. n=4–9 per group. *: $p<0.05$; **: $p<0.01$; ***: $p<0.001$.

CatS is also a key feature of the pulmonary disease of βENaC-Tg mice, a model of CF-like lung disease. The βENaC-Tg mouse provides a relevant model for investigating CF lung disease pathogenesis, particularly the interactions between ion transport, airway surface liquid and mucociliary clearance [13, 14]. However, because CF transmembrane conductance regulator (CFTR) function is normal in the βENaC-Tg mouse lung [13], this model does not allow the study of pathophysiological changes associated directly with mutant CFTR, such as cellular dysfunction and mucus composition. Knockdown of CatS by pharmacological (VBY-999 inhibitor) or genetic methods (CatS$^{-/-}$) in the βENaC-Tg model resulted in a significant decline in both lung macrophage and neutrophil cell populations, providing further evidence of a role for CatS in mediating pulmonary inflammation [30–32].

Previous work in βENaC-Tg mice demonstrated that genetic knockdown of neutrophil elastase and matrix metalloproteinase 12 significantly reduced structural lung damage, but had no effect on mucus obstruction and pulmonary mortality [33, 34]. In this study, pharmacological inhibition and genetic ablation of CatS not only led to reduced airway structural damage and pulmonary inflammation, but also ameliorated airway mucus plugging and improved survival rates of neonatal mice. These data indicate the involvement of CatS in inflammatory cell recruitment, lung tissue damage and the development of mucus plugging. In agreement, we have also shown that direct administration of CatS to the lungs of WT mice induced neutrophil recruitment and increased KC levels in the lungs of these mice. Pulmonary CatS instillation resulted in significantly increased expression of the mucin Muc5ac and Gob5, a marker associated with goblet cell hyperplasia [35, 36], as well as the number of goblet cells and mucus-producing cells, although no effect on Muc5b expression was observed. These results indicate a role for CatS-mediated lung
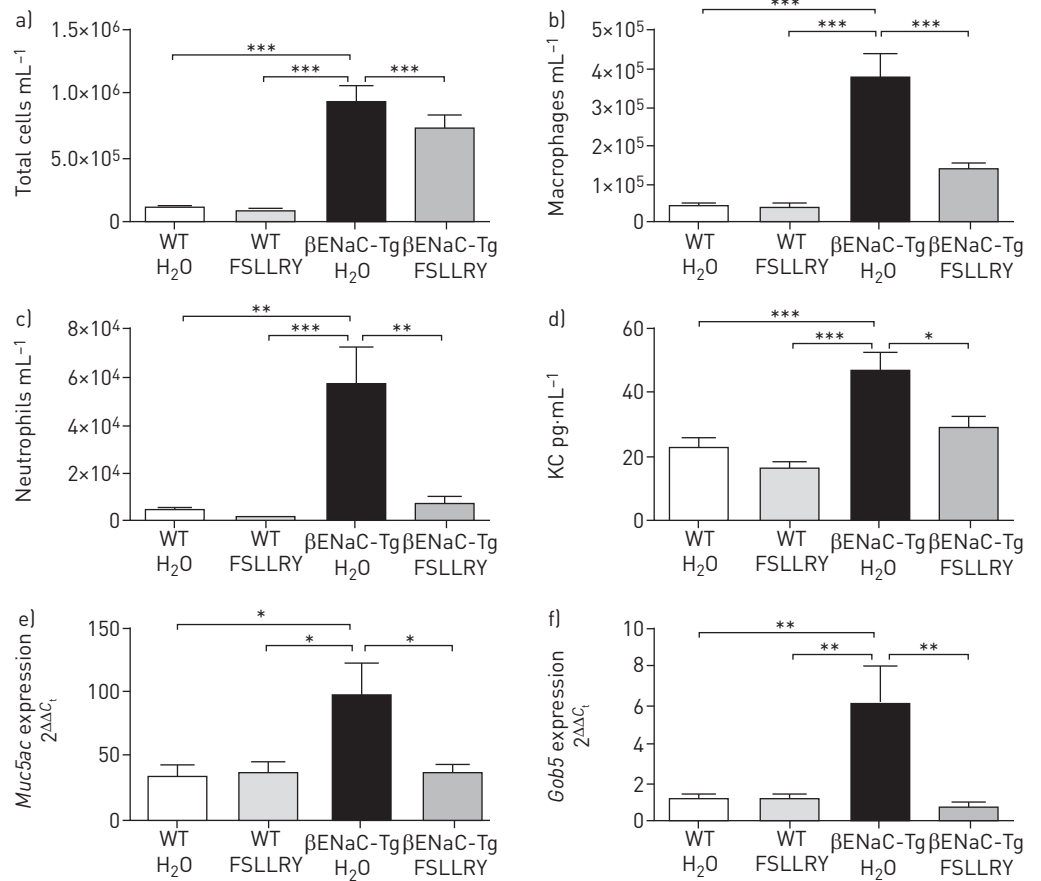
FIGURE 8 Protease-activated receptor 2 (PAR2) inhibition reduces airway inflammation in β-epithelial Na$^+$ channel-overexpressing transgenic (βENaC-Tg) mice. WT: wild-type; H$_2$O: sterile water; FSLLRY: FSLLRY-NH$_2$. WT and βENaC-Tg mice were treated daily with the PAR2 peptide antagonist FSLLRY (4 mg·kg^{-1}) or vehicle control (H$_2$O) for 14 days. Bronchoalveolar lavage a) total cell, b) macrophage and c) neutrophil counts, and d) chemokine KC levels were quantified. n=6–11 per group. Expression levels of e) *Muc5ac* and f) *Gob5* in lung tissue were analysed by quantitative PCR. n=9 per group. *: p<0.05; **: p<0.01; ***: p<0.001.

inflammation in the CF lung, and suggest that CatS may contribute to airway mucus plugging *via* goblet cell hyperplasia and increased mucus production.

These effects may be due, in part, to the activation of PAR2 by CatS, which has previously been demonstrated in other organ systems outside of the lung [15–20]. Research to date suggests that PAR2 activation is associated with inflammation, leukocyte recruitment and mucin expression [37–40]. In this study we have shown that antagonism of PAR2 led to a reduction in the inflammatory cell infiltrate in the lungs of mice exposed to CatS as well as in the βENaC-Tg lung. In addition, reductions in BAL fluid KC levels and expression levels of Muc5ac and Gob5 were also observed in PAR2 antagonist-treated βENaC-Tg mice. In agreement with previous reports, our data suggest that CatS may exert its effects on pulmonary inflammation and mucus plugging, at least in part, *via* PAR2. In contrast, while knockdown or inhibition of CatS reduced lung tissue destruction in βENaC-Tg mice, we did not observe a reduction in lung damage (Lm or DI) in PAR2 antagonist-treated βENaC-Tg mice, suggesting that CatS may be acting *via* other pathways to elicit lung damage. For example, we have shown that direct instillation of CatS into the WT mouse lung can rapidly induce (within 24 h) desmosine levels in BAL fluid, indicating that the effects of CatS may also be mediated directly on lung tissue as well as *via* PAR2.

In summary, our investigations show that CatS is elevated in an *in vivo* model of CF-like lung disease, and may promote pulmonary cell infiltration, mucus obstruction and structural lung damage associated with chronic lung diseases such as CF. These results suggest that CatS may play a vital role in CF-like lung disease pathogenesis, which ultimately leads to the loss of tissue structural integrity and lung function. As previously mentioned, CatS possesses the ability to cleave and inactivate host antimicrobial proteins [4, 9–12], which may increase susceptibility to infection in patients with muco-obstructive lung diseases such as

CF and COPD. However, further work is needed to investigate the impact of elevated CatS activity and the effects of pulmonary CatS inhibition on *Pseudomonas* infection in the context of chronic lung disease. Our results indicate that CatS may be a promising therapeutic target to halt the progression of airway inflammation, mucus obstruction and pulmonary damage associated with CF lung disease.

References

1   Riese RJ, Mitchell RN, Villadangos JA, et al. Cathepsin S activity regulates antigen presentation and immunity. *J Clin Invest* 1998; 101: 2351–2363.
2   Shi GP, Munger JS, Meara JP, et al. Molecular cloning and expression of human alveolar macrophage cathepsin S, an elastinolytic cysteine protease. *J Biol Chem* 1992; 267: 7258–7262.
3   Brömme D, Bonneau PR, Lachance P, et al. Functional expression of human cathepsin S in *Saccharomyces cerevisiae*. Purification and characterization of the recombinant enzyme. *J Biol Chem* 1993; 268: 4832–4838.
4   Taggart CC, Greene CM, Smith SG, et al. Inactivation of human beta-defensins 2 and 3 by elastolytic cathepsins. *J Immunol* 2003; 171: 931–937.
5   Martin SL, Moffitt KL, McDowell A, et al. Association of airway cathepsin B and S with inflammation in cystic fibrosis. *Pediatr Pulmonol* 2010; 45: 860–868.
6   Naudin C, Joulin-Giet A, Couetdic G, et al. Human cysteine cathepsins are not reliable markers of infection by *Pseudomonas aeruginosa* in cystic fibrosis. *PLoS One* 2011; 6: e25577.
7   Weldon S, McNally P, McAuley DF, et al. miR-31 dysregulation in cystic fibrosis airways contributes to increased pulmonary cathepsin S production. *Am J Respir Crit Care Med* 2014; 190: 165–174.
8   Geraghty P, Greene CM, O'Mahony M, et al. Secretory leucocyte protease inhibitor inhibits interferon-gamma-induced cathepsin S expression. *J Biol Chem* 2007; 282: 33389–33395.
9   Rogan MP, Taggart CC, Greene CM, et al. Loss of microbicidal activity and increased formation of biofilm due to decreased lactoferrin activity in patients with cystic fibrosis. *J Infect Dis* 2004; 190: 1245–1253.
10   Andrault P-M, Samsonov SA, Weber G, et al. Antimicrobial peptide LL-37 is both a substrate of cathepsins S and K and a selective inhibitor of cathepsin L. *Biochemistry* 2015; 54: 2785–2798.
11   Lecaille F, Naudin C, Sage J, et al. Specific cleavage of the lung surfactant protein A by human cathepsin S may impair its antibacterial properties. *Int J Biochem Cell Biol* 2013; 45: 1701–1709.
12   Taggart CC, Lowe GJ, Greene CM, et al. Cathepsin B, L, and S cleave and inactivate secretory leucoprotease inhibitor. *J Biol Chem* 2001; 276: 33345–33352.
13   Mall M, Grubb BR, Harkema JR, et al. Increased airway epithelial Na$^+$ absorption produces cystic fibrosis-like lung disease in mice. *Nat Med* 2004; 10: 487–493.
14   Zhou Z, Duerr J, Johannesson B, et al. The ENaC-overexpressing mouse as a model of cystic fibrosis lung disease. *J Cyst Fibros* 2011; 10: S172–S182.
15   Tato M, Kumar SV, Liu Y, et al. Cathepsin S inhibition combines control of systemic and peripheral pathomechanisms of autoimmune tissue injury. *Sci Rep* 2017; 7: 2775.
16   Reddy VB, Shimada SG, Sikand P, et al. Cathepsin S elicits itch and signals via protease-activated receptors. *J Invest Dermatol* 2010; 130: 1468–1470.
17   Kumar VR S, Darisipudi MN, Steiger S, et al. Cathepsin S cleavage of protease-activated receptor-2 on endothelial cells promotes microvascular diabetes complications. *J Am Soc Nephrol* 2016; 27: 1635–1649.
18   Kim N, Bae KB, Kim MO, et al. Overexpression of cathepsin S induces chronic atopic dermatitis in mice. *J Invest Dermatol* 2012; 132: 1169–1176.
19   Cattaruzza F, Lyo V, Jones E, et al. Cathepsin S is activated during colitis and causes visceral hyperalgesia by a PAR2-dependent mechanism in mice. *Gastroenterology* 2011; 141: 1864–1874.
20   Lee TK-W, Cheung VC-H, Lu P, et al. Blockade of CD47-mediated cathepsin S/protease-activated receptor 2 signaling provides a therapeutic target for hepatocellular carcinoma. *Hepatology* 2014; 60: 179–191.
21   Johannesson B, Hirtz S, Schatterny J, et al. CFTR regulates early pathogenesis of chronic obstructive lung disease in βENaC-overexpressing mice. *PLoS One* 2012; 7: e44059.

22   Shi GP, Villadangos JA, Dranoff G, *et al.* Cathepsin S required for normal MHC class II peptide loading and germinal center development. *Immunity* 1999; 10: 197–206.

23   Small DM, Zani M-L, Quinn DJ, *et al.* A functional variant of elafin with improved anti-inflammatory activity for pulmonary inflammation. *Mol Ther* 2015; 23: 24–31.

24   Saetta M, Shiner RJ, Angus GE, *et al.* Destructive index: a measurement of lung parenchymal destruction in smokers. *Am Rev Respir Dis* 1985; 131: 764–769.

25   Dunnill MS. Quantitative methods in the study of pulmonary pathology. *Thorax* 1962; 17: 320–328.

26   Mall MA, Harkema JR, Trojanek JB, *et al.* Development of chronic bronchitis and emphysema in beta-epithelial Na$^+$ channel-overexpressing mice. *Am J Respir Crit Care Med* 2008; 177: 730–742.

27   Sevenich L, Bowman RL, Mason SD, *et al.* Analysis of tumour- and stroma-supplied proteolytic networks reveals a brain-metastasis-promoting role for cathepsin S. *Nat Cell Biol* 2014; 16: 876–888.

28   Gupta S, Singh RK, Dastidar S, *et al.* Cysteine cathepsin S as an immunomodulatory target: present and future trends. *Expert Opin Ther Targets* 2008; 12: 291–299.

29   Small DM, Burden RE, Scott CJ. The emerging relevance of the cysteine protease cathepsin S in disease. *Clin Rev Bone Miner Metab* 2011; 9: 122–132.

30   Williams AS, Eynott PR, Leung S-Y, *et al.* Role of cathepsin S in ozone-induced airway hyperresponsiveness and inflammation. *Pulm Pharmacol Ther* 2009; 22: 27–32.

31   Hirakawa H, Pierce RA, Bingol-Karakoc G, *et al.* Cathepsin S deficiency confers protection from neonatal hyperoxia-induced lung injury. *Am J Respir Crit Care Med* 2007; 176: 778–785.

32   Zheng T, Kang MJ, Crothers K, *et al.* Role of cathepsin S-dependent epithelial cell apoptosis in IFN-gamma-induced alveolar remodeling and pulmonary emphysema. *J Immunol* 2005; 174: 8106–8115.

33   Gehrig S, Duerr J, Weitnauer M, *et al.* Lack of neutrophil elastase reduces inflammation, mucus hypersecretion, and emphysema, but not mucus obstruction, in mice with cystic fibrosis-like lung disease. *Am J Respir Crit Care Med* 2014; 189: 1082–1092.

34   Trojanek JB, Cobos-Correa A, Diemer S, *et al.* Airway mucus obstruction triggers macrophage activation and matrix metalloproteinase 12-dependent emphysema. *Am J Respir Cell Mol Biol* 2014; 51: 709–720.

35   Long AJ, Sypek JP, Askew R, *et al.* Gob-5 contributes to goblet cell hyperplasia and modulates pulmonary tissue inflammation. *Am J Respir Cell Mol Biol* 2006; 35: 357–365.

36   Morton JD, Alevy YG, Peltz G, *et al.* Functional genomics of asthma: role of CLCA3 in goblet cell metaplasia (GCM) but not airway hyperreactivity (AHR). *J Allergy Clin Immunol* 2004; 113: S205.

37   Bonnart C, Feuillet G, Vasseur V, *et al.* Protease-activated receptor 2 contributes to *Toxoplasma gondii*-mediated gut inflammation. *Parasite Immunol* 2017; 39: e12489.

38   Nichols HL, Saffeddine M, Theriot BS, *et al.* β-Arrestin-2 mediates the proinflammatory effects of proteinase-activated receptor-2 in the airway. *Proc Natl Acad Sci USA* 2012; 109: 16660–16665.

39   Chin AC, Lee WY, Nusrat A, *et al.* Neutrophil-mediated activation of epithelial protease-activated receptors-1 and -2 regulates barrier function and transepithelial migration. *J Immunol* 2008; 181: 5702–5710.

40   Asaduzzaman M, Nadeem A, Arizmendi N, *et al.* Functional inhibition of PAR2 alleviates allergen-induced airway hyperresponsiveness and inflammation. *Clin Exp Allergy* 2015; 45: 1844–1855.